EUROPEAN ORGANISATION FOR NUCLEAR RESEARCH (CERN)

July 8, 2024

Supplemental Material for: Determination of the relative sign of the Higgs boson couplings to W and Z bosons using WH production via vector-boson fusion with the ATLAS detector

The ATLAS Collaboration

This supplemental material presents details on the results, including limits on the signal strength for the negative- and positive-λ_{WZ} analyses, and separate exclusion contours for the present analysis and the combination of previous Higgs boson measurements [2]. In addition, the data are compared to predictions for the event yields in the analysis regions, and for key kinematic distributions in the signal regions. Finally, tables are shown detailing the sources of uncertainty and the correlations among the fit parameters.

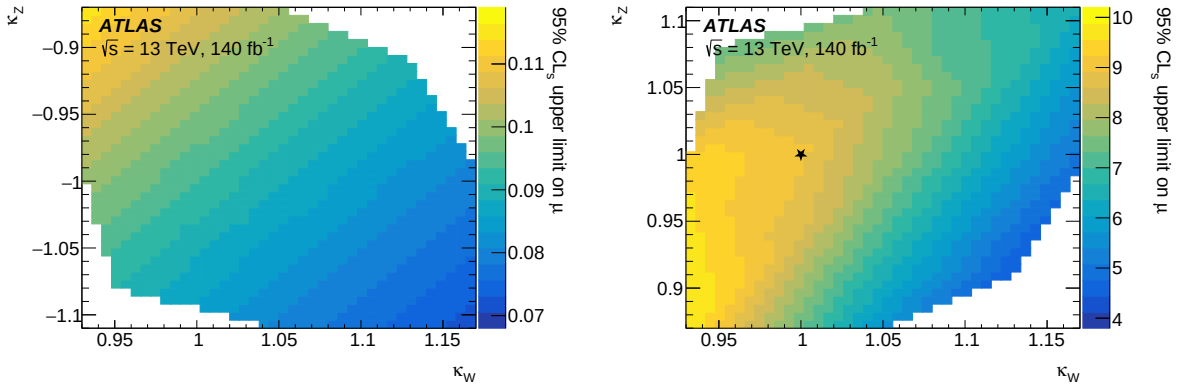

Figure 1: Exclusion limits at 95% CL_s on the signal strength for VBF WH production for different values of κ_W and κ_Z. Negative values of λ_{WZ} are on the left, and positive values are on the right. The Standard Model is indicated with a star. The white regions are excluded at greater than 95% confidence level by other ATLAS Higgs boson measurements [2], and do not have simulated signal predictions.

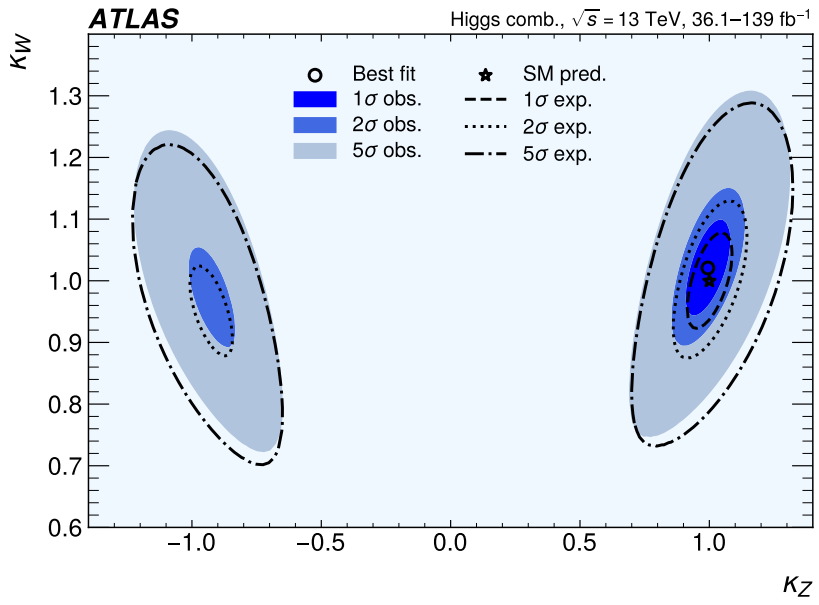

Figure 2: Fit results in the (κ_Z, κ_W) plane, using a combination of previous Higgs boson measurements [2]. The fit assumes that all Higgs boson couplings besides the ones plotted are positive, and that only SM particles contribute to loop processes. Confidence regions are constructed based on the log-likelihood ratio $\Lambda_{\mathrm{LR}} = -2\ln(L/L_{\mathrm{max}})$, where L_{max} is the likelihood for the best fit point, which is shown as a black circle. The 1σ, 2σ and 5σ regions are defined by Λ_{LR} values smaller than 2.30, 6.18, and 28.7, respectively. Negative values of κ_W are excluded with significance greater than 5σ, primarily due to interference between the W boson and top quark contributions to the loop decay $H \to \gamma\gamma$. The SM value is marked with a star.

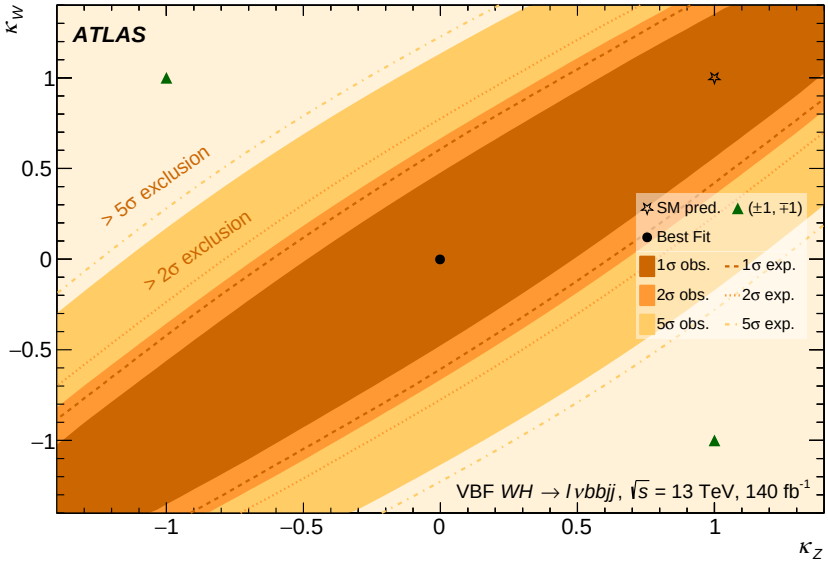

Figure 3: Fit results in the (κ_Z, κ_W) plane, using the negative λ_{WZ} analysis. Confidence regions are constructed based on the log-likelihood ratio $\Lambda_{\mathrm{LR}} = -2\ln(L/L_{\mathrm{max}})$, where L_{max} is the likelihood for the best fit point, which is shown as a black dot. The 1σ, 2σ and 5σ regions are defined by Λ_{LR} values smaller than 2.30, 6.18, and 28.7, respectively. The SM value is marked with a star, while green triangles mark the points with $\kappa_Z = \pm 1$, $\kappa_W = \mp 1$.

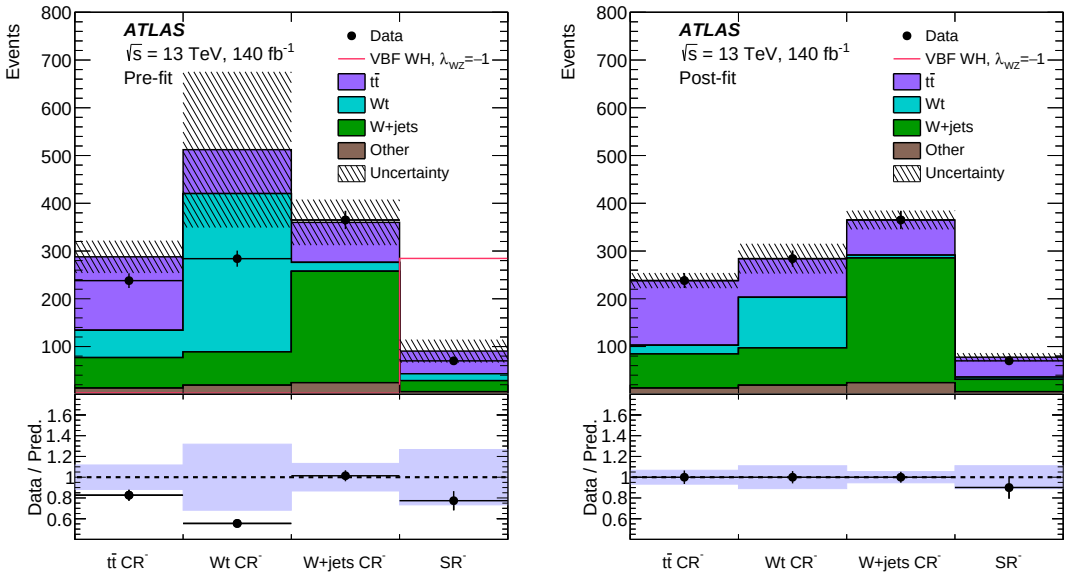

Figure 4: Data compared to the background prediction in each region of the negative λ_{WZ} analysis, before (left) and after (right) the fit to data. The signal prediction with $\kappa_W = +1$, $\kappa_Z = -1$ is shown overlaid in the pre-fit plot. The fitted signal strength is $\hat{\mu} = -0.027$, corresponding to -8 events. This contribution is not shown in the figure. The predicted signal yield with $\kappa_W = +1$, $\kappa_Z = +1$ in SR^- is 2.93 events, which is also not shown in the figure. The shaded bands represent the total pre- or post-fit uncertainty on the prediction. The pre-fit uncertainty does not include the normalization of the main backgrounds, which is unconstrained in the fit.

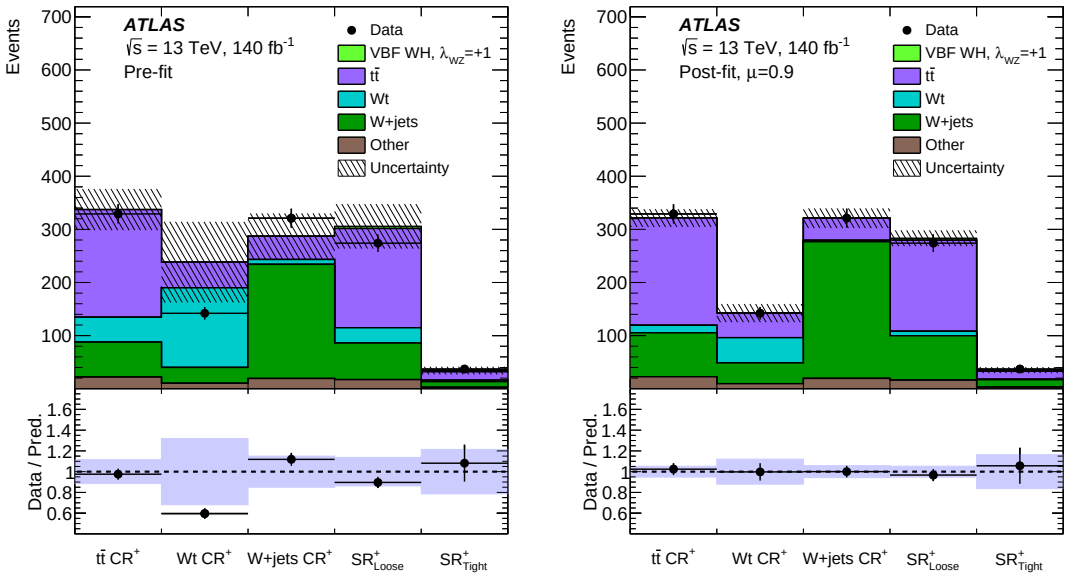

Figure 5: Data compared to the SM prediction in each region of the positive λ_{WZ} analysis, before (left) and after (right) the fit to data. The shaded bands represent the total pre- or post-fit uncertainty on the prediction. The pre-fit uncertainty does not include the normalization of the main backgrounds, which is unconstrained in the fit.

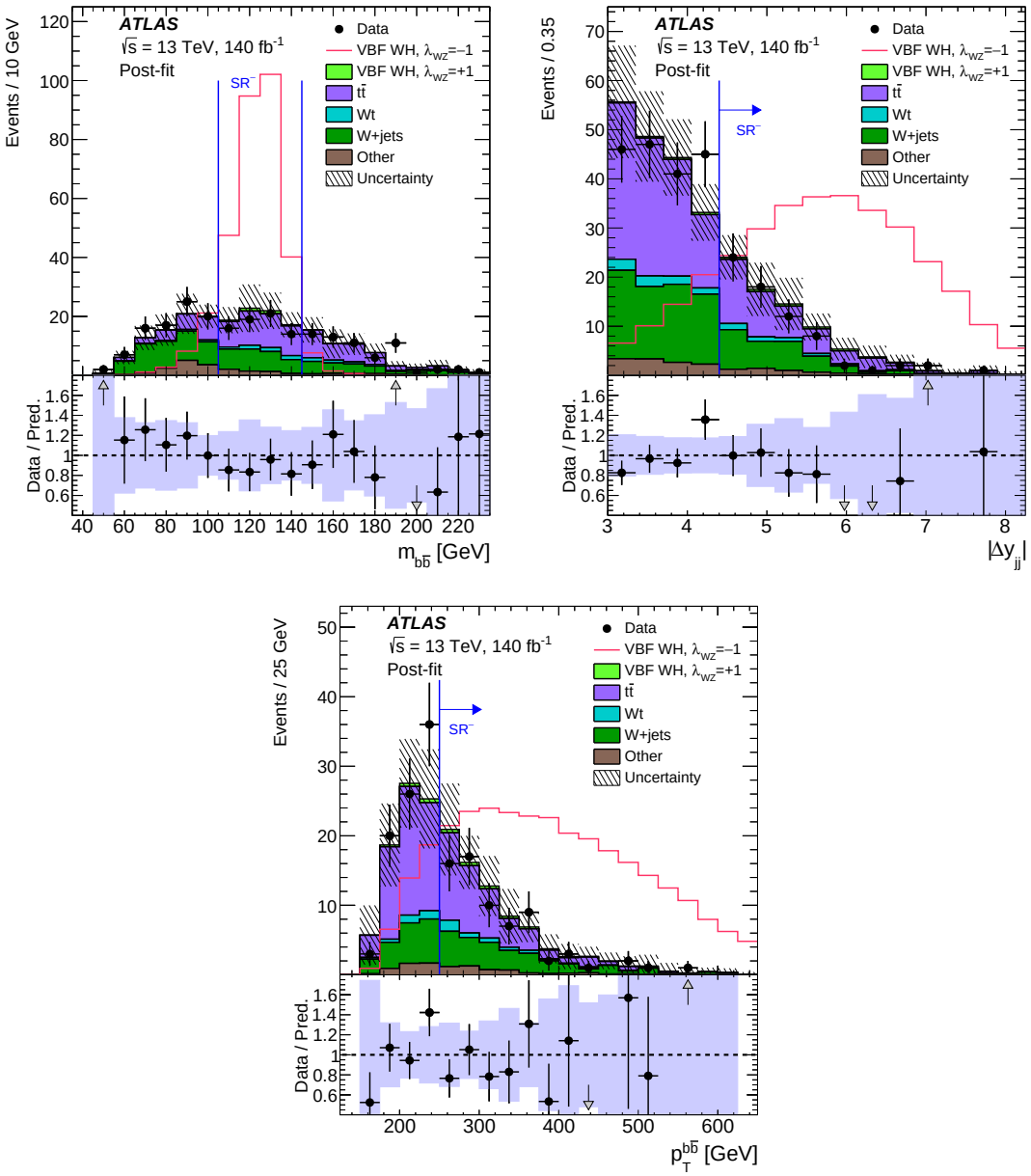

Figure 6: Data compared to the SM prediction for $m_{b\bar{b}}$, $|\Delta y_{jj}|$, and $p_{\mathrm{T}}^{b\bar{b}}$ in the negative λ_{WZ} analysis. The background yields are scaled to the post-fit prediction. The SM signal with $\kappa_W = +1$, $\kappa_Z = +1$ is shown as part of the stacked prediction, while the BSM signal with $\kappa_W = +1$, $\kappa_Z = -1$ is presented separately. For each figure, all of the cuts used to define SR^- are applied, except for the cut on the represented variable. These cuts are indicated with a blue line. The shaded bands represent the total post-fit uncertainty on the prediction.

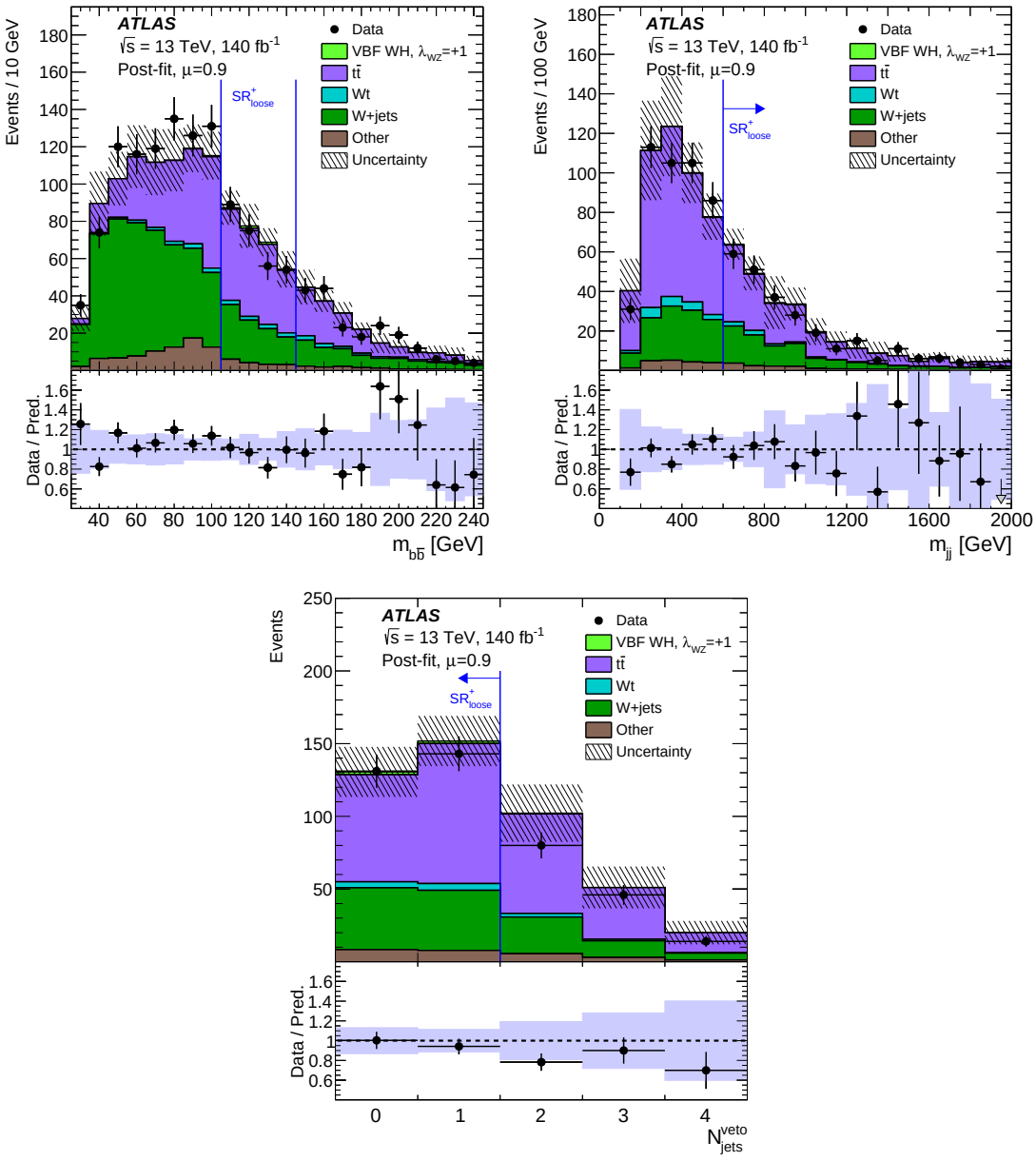

Figure 7: Data compared to the SM prediction for $m_{b\bar{b}}$, m_{jj}, and $N_{\text{jets}}^{\text{veto}}$ in the positive λ_{WZ} analysis. The background yields are scaled to the post-fit prediction, while the signal is scaled to the fitted signal strength $\mu = 2.6$. For each figure, all of the cuts used to define $\text{SR}^{+}_{\text{loose}}$ are applied, except for the cut on the represented variable. These cuts are indicated with a blue line. The shaded bands represent the total post-fit uncertainty on the prediction.

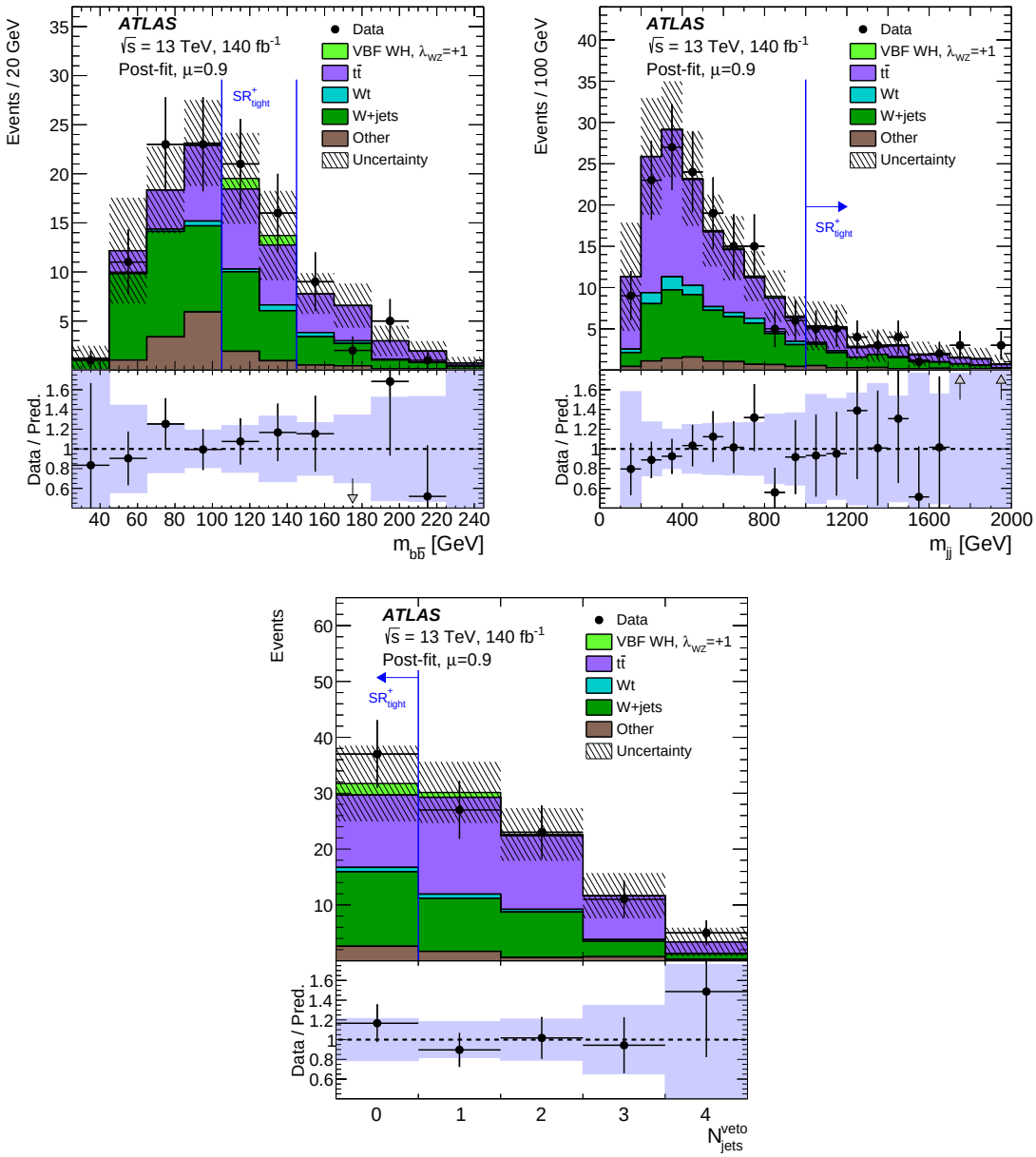

Figure 8: Data compared to the SM prediction for $m_{b\bar{b}}$, m_{jj}, and $N_{\text{jets}}^{\text{veto}}$ in the positive λ_{WZ} analysis. The background yields are scaled to the post-fit prediction, while the signal is scaled to the fitted signal strength $\mu = 2.6$. For each figure, all of the cuts used to define $\text{SR}_{\text{tight}}^{+}$ are applied, except for the cut on the represented variable. These cuts are indicated with a blue line. The shaded bands represent the total post-fit uncertainty on the prediction.

Uncertainty source	$\Delta\mu$
$t\bar{t}$ modelling	± 0.033
Jet energy resolution	± 0.017
Wt modelling	± 0.013
Jet energy scale	± 0.011
Signal modelling	± 0.007
W+jets modelling	± 0.006
MC statistical uncertainty	± 0.005
Jet vertex tagging	± 0.003
Flavor tagging	± 0.002
$E_{\mathrm{T}}^{\mathrm{miss}}$ scale and trigger efficiency	± 0.001
Luminosity and pileup reweighting	± 0.001
Other background modelling	± 0.001
Lepton scale and efficiency	< 0.001
Total systematic	± 0.045
Normalization factors	± 0.016
Total statistical	± 0.032
Total uncertainty	± 0.055

Table 1: Contribution of different sources of uncertainty to the total uncertainty on μ, in the negative λ_{WZ} analysis. In the case of asymmetric uncertainties, the average of the positive and negative variations is given.

Uncertainty source	$\Delta\mu$
W+jets modelling	± 1.9
$t\bar{t}$ modelling	± 1.8
Jet energy resolution	± 1.3
Jet energy scale	± 0.8
MC statistical uncertainty	± 0.8
Other background modelling	± 0.5
Signal modelling	± 0.4
Wt modelling	± 0.3
$E_{\mathrm{T}}^{\mathrm{miss}}$ scale and trigger efficiency	± 0.3
Flavor tagging	± 0.1
Luminosity and pileup reweighting	± 0.1
Jet vertex tagging	± 0.1
Lepton scale and efficiency	< 0.1
Total systematic	± 3.3
Normalization factors	± 1.4
Total statistical	± 2.5
Total uncertainty	± 4.1

Table 2: Contribution of different sources of uncertainty to the total uncertainty on μ, in the positive λ_{WZ} analysis. In the case of asymmetric uncertainties, the average of the positive and negative variations is given.

	k_W	k_{Wt}	$k_{t\bar{t}}$	μ
k_W	1.00			
k_{Wt}	0.02	1.00		
$k_{t\bar{t}}$	−0.71	−0.31	1.00	
μ	0.14	−0.19	−0.16	1.00

Table 3: Correlation coefficients among the unconstrained parameters in the negative λ_{WZ} analysis.

	k_W	k_{Wt}	$k_{t\bar{t}}$	μ
k_W	1.00			
k_{Wt}	−0.06	1.00		
$k_{t\bar{t}}$	−0.54	−0.22	1.00	
μ	−0.31	0.16	0.08	1.00

Table 4: Correlation coefficients among the unconstrained parameters in the positive λ_{WZ} analysis.